

Exploring nonlinear topological states of matter with exciton-polaritons: Edge solitons in kagome lattice

D. R. Gulevich^{1,2,*}, D. Yudin^{1,3}, D. V. Skryabin^{1,2}, I. V. Iorsh^{1,3}, and I. A. Shelykh^{1,4}

¹ITMO University, St. Petersburg 197101, Russia

²Department of Physics, University of Bath, Bath BA2 7AY, United Kingdom

³Division of Physics and Applied Physics, Nanyang Technological University 637371, Singapore

⁴Science Institute, University of Iceland, Dunhagi 3, IS-107, Reykjavik, Iceland

ABSTRACT

Matter in nontrivial topological phase possesses unique properties, such as support of unidirectional edge modes on its interface. It is the existence of such modes which is responsible for the wonderful properties of a topological insulator – material which is insulating in the bulk but conducting on its surface, along with many of its recently proposed photonic and polaritonic analogues. We show that exciton-polariton fluid in a nontrivial topological phase in kagome lattice, supports nonlinear excitations in the form of solitons built up from wavepackets of topological edge modes – topological edge solitons. Our theoretical and numerical results indicate the appearance of bright, dark and grey solitons dwelling in the vicinity of the boundary of a lattice strip. In a parabolic region of the dispersion the edge solitons can be described by envelope functions with profiles defined by solutions of the nonlinear Schrödinger equation. Topological edge solitons thus remain undisturbed under disorder scattering which proves them to be true solitons as opposed to solitary waves for which such requirement is waived. Importantly, the kagome lattice supports topological edge modes with zero group velocities unlike other types of truncated lattices.

Introduction

Various physical systems often demonstrate similarity in the underlying physical phenomena, which drives an idea of exploiting the well controllable systems for mimicking properties of the less controllable and less accessible ones. The spectacular example is the analogy between electronic and photonic systems¹. It is therefore not surprising that with the fast rise of topological insulators in the electronic systems^{2–4}, topological ideas had been simultaneously explored in photonic systems. Among the pioneering works are the study of chiral edge states in photonic crystals⁵ where the Berry curvature for photonic bands was introduced by analogy with electronic systems, photonic analogues of Hall effect^{6–8} and analogues of topological insulators^{9–12}, as well as a solid number of both theoretical and experimental works demonstrating the effects of non-trivial topology in the electromagnetic systems in the spectral range from radio to optical frequencies¹³.

Despite this success, however, the optical circuits are not well suited for nonlinear effects to be directly incorporated while breaking of the time-reversal symmetry which is needed to induce topological states, remains a challenging task. In this respect, systems based on exciton-polaritons¹⁴, quasi-particles originating from the strong coupling of the quantum well-excitons and cavity photons in the microcavities, are at advantage. Being hybrid light-matter excitations, photonic properties of exciton-polaritons allow for them to be effectively controlled with the use of optical potential profile, while their excitonic nature brings significant interactions and a strong nonlinear response^{15–18}. Moreover, due to the exciton spin, the time-reversal symmetry of an exciton-polariton system can be easily broken by application of the external magnetic field. This makes polaritonic systems attractive both from the point of view of applications in prospective polaritonic devices^{19,20} as well as a unique laboratory to simulate the topological properties of matter.

There had been a few proposals for creating topologically nontrivial states of polaritons. In the last few years, emergence of the non-trivial topology and existence of the topologically protected edge states in the polaritonic lattices of different geometry were already addressed in a number of studies^{21–27}. It is, therefore, natural, that the focus of attention in the study of the effects of non-trivial topology has shifted towards systems with nonlinearity, where exciton-polaritons play an important role. Among the recent works where the interplay of the nonlinear effects with nontrivial topology has been explored are studies of self-localized states^{28,29}, self-induced topological transitions³⁰, topological Bogoliubov excitations²⁵, vortices in lattices³¹, Meissner states in ring resonators³² and solitons in lattices^{33–36}. In Ref. 27 it has been recently observed that in a certain range of parameters kagome lattice possesses a highly nonlinear dispersion of the topological edge states, with well pronounced minimum and maximum inside the bulk gap. In the present paper we show that such peculiar dispersion shape leads to the appearance of the nonlinear edge excitations in the form of the solitons which are robust under disorder scattering

and soliton-soliton collisions. Such excitations thus turn out to be true solitons as opposed to solitary waves for which the requirement of restoring shape upon collision is usually waived³⁷. In contrast to solitons in the honeycomb lattice³⁵ the group velocity of topological edge state solitons can change sign and can be efficiently tuned in the wide range by changing of the central quasi-momentum of the wavepacket.

Results

Model of Polaritonic Kagome Lattice

In the tight-binding approximation the Hamiltonian for polaritons confined to an array of coupled microcavity pillars arranged into a kagome lattice reads

$$\hat{H} = \Omega \sum_{i,\sigma} \sigma \hat{a}_{i,\sigma}^\dagger \hat{a}_{i,\sigma} - \sum_{\langle ij \rangle, \sigma} \left(J \hat{a}_{i,\sigma}^\dagger \hat{a}_{j,\sigma} + \delta J e^{2i\phi_{ij}\sigma} \hat{a}_{i,\sigma}^\dagger \hat{a}_{j,\bar{\sigma}} + h.c. \right) + \sum_{i,\sigma} \left(\frac{\alpha_1}{2} \hat{a}_{i,\sigma}^\dagger \hat{a}_{i,\sigma} \hat{a}_{i,\sigma}^\dagger \hat{a}_{i,\sigma} + \alpha_2 \hat{a}_{i,\sigma}^\dagger \hat{a}_{i,\sigma} \hat{a}_{i,\bar{\sigma}}^\dagger \hat{a}_{i,\bar{\sigma}} \right) \quad (1)$$

Equation (1) is generalization of the linear model studied in Ref. 27 to account for the polariton-polariton interactions. Here, operators $\hat{a}_{i,\sigma}^\dagger$ ($\hat{a}_{i,\sigma}$) create (annihilate) exciton-polariton of circular polarization $\sigma = \pm$ at site i of the kagome lattice, the summation $\langle ij \rangle$ is over nearest neighbors (NN), angles ϕ_{ij} specify directions of vectors connecting the neighboring sites. The first term in (1) describes the Zeeman energy splitting (2Ω) of the circular polarized components induced by external magnetic field, the second term describes the NN hopping with conservation and inversion of circular polarization (the latter comes from TE-TM splitting), and the last term describes the on-site polariton-polariton interactions with effective constants α_1 and α_2 defined for the involved pillar mode. In what follows, we will use normalized units where J is a unit energy and the interpillar distance is the unit length (size of the kagome lattice unit cell then equals 2 in this units, see Fig. 1a).

In the linear regime when the interactions in (1) can be neglected, the band structure of polaritonic kagome lattice was calculated in Ref. 27. There, it was shown that presence of finite TE-TM splitting δJ and magnetic field Ω opens a gap which separates the Bloch bands into two bundles, each possessing a nontrivial topology. As known from the theory of topological insulators, the bulk-boundary correspondence then suggests that there must exist topological edge modes (TEM) propagating along the interface of a finite (or, semi-finite) lattice. While the number of TEM is a topological invariant and thus is independent of the type of a boundary, the very dispersion of the TEM does depend on how the lattice is cut at its interface. The boundary with a line of pillar uncoupled between each other (see, the bottom edge of the strip in Fig. 1a) is more prone to localization and thus generally exhibits flatter dispersions of TEM than those where the sites are directly connected via NN coupling (e.g. the top edge on Fig. 1a). Furthermore, the sign of the group velocity of the edge states propagating along the “uncoupled” boundary (the bottom one on Fig. 1a) can be reversed, see Fig. 1b. Such highly nonlinear dispersion turns out to be favorable for the existence of nonlinear excitations of TEM in the form of edge solitons. In the following sections we will show that this is indeed the case and present our analytic and numerical results.

Theory of nonlinear topological edge excitations in a 2D lattice

To study the nonlinear topological edge excitations we employ the mean field approximation. We consider a strip of kagome lattice with M sites in its unit cell, see Fig. 1a and introduce vectors $\Psi_m^\sigma = (\psi_{m,1}^\sigma, \dots, \psi_{m,M}^\sigma)^T$ composed of the spinor components $\sigma = \pm$ at each site of the m th unit cell, where index m enumerates the unit cells in the x direction (see Fig. 1a). Then, the time evolution of the m th vector is described by the coupled system of the Gross-Pitaevskii equations reads

$$i\partial_t \Psi_m^\sigma = \sum_\tau (\hat{H}_{-1}^{\sigma,\tau} \Psi_{m-1}^\tau + \hat{H}_0^{\sigma,\tau} \Psi_m^\tau + \hat{H}_{+1}^{\sigma,\tau} \Psi_{m+1}^\tau) + \hat{N}^\sigma(\Psi_m^+, \Psi_m^-) \Psi_m^\sigma, \quad (2)$$

where $\hat{N}^\sigma(\Psi_m^+, \Psi_m^-)$ is the diagonal matrix with elements

$$[\hat{N}^\sigma(\Psi_m^+, \Psi_m^-)]_{ij} = \delta_{i,j} (|\psi_{m,j}^\sigma|^2 + \alpha |\psi_{m,j}^{\bar{\sigma}}|^2),$$

parameter $\alpha \equiv \alpha_2/\alpha_1$, and Ψ_m^σ are normalized to $\sum_{\sigma,m} \langle \Psi_m^\sigma, \Psi_m^\sigma \rangle \equiv \sum_{\sigma,m,j} [\Psi_m^\sigma]_j [\Psi_m^\sigma]_j = NJ/\alpha_1$ with N being the total number of polaritons in the system. Matrices $\hat{H}_j^{\sigma,\tau}$, satisfy $(\hat{H}_j^{\sigma,\tau})^\dagger = \hat{H}_{-j}^{\tau,\sigma}$ for all $\sigma, \tau = \pm, j = 0, \pm 1$, which ensures hermiticity of the Hamiltonian. In the absence of interactions the stationary states of (2) are Bloch waves $e^{-i\mu t + ikLm} \mathbf{u}_k^\sigma$ where L is the spatial extent of the unit cell in the x direction and \mathbf{u}_k^σ are m -independent solutions to the eigenvalue problem

$$\sum_\tau \left(e^{-ikL} \hat{H}_{-1}^{\sigma,\tau} + \hat{H}_0^{\sigma,\tau} + e^{ikL} \hat{H}_{+1}^{\sigma,\tau} \right) \mathbf{u}_{k,n}^\tau = \mu_{k,n} \mathbf{u}_{k,n}^\sigma \quad \text{for } \sigma = \pm, \quad (3)$$

where n enumerated the energy bands. Because the operator in the left hand side of (3) is self-adjoint, $\mathbf{u}_k^{\sigma,n}$ forms orthonormal set,

$$\sum_\sigma \langle \mathbf{u}_{k,n}^\sigma, \mathbf{u}_{k,m}^\sigma \rangle = \sum_{\sigma,j} [\mathbf{u}_{k,n}^{\sigma*}]_j [\mathbf{u}_{k,m}^\sigma]_j = \delta_{n,m}.$$

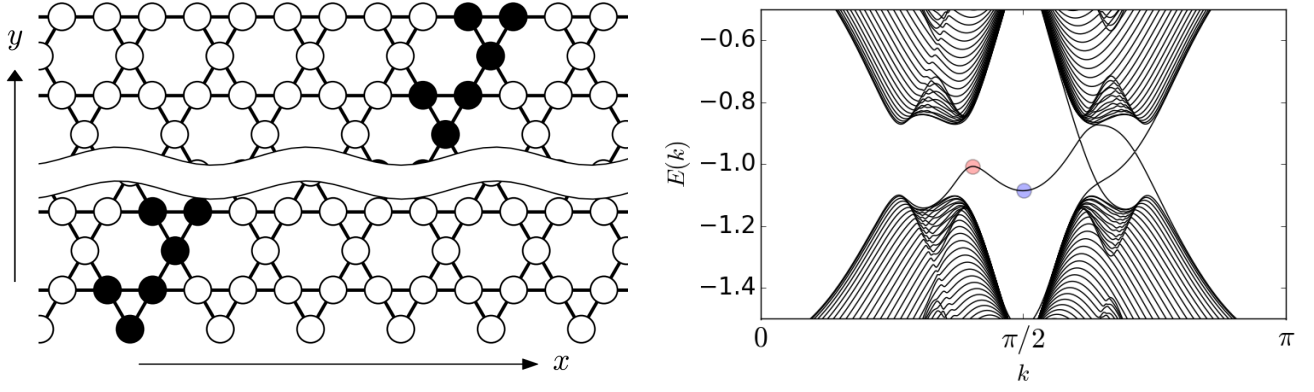


Figure 1. (a) A strip of kagome lattice. The strip is infinite along x but has a finite extent along the y axis. The sites marked by black form a unit cell of the strip. The bottom boundary of the strip with a row of uncoupled sites supports the dispersion of topological edge mode with the group velocity changing sign within the bulk gap as shown in Figure b. (b) Dispersion of topological edge modes propagating in a strip of kagome lattice. Dispersion of edge states with reversed group velocity and a well defined minimum and maximum lying within the bulk gap appears for a certain range of values of the magnetic field and TE-TM splitting (in this example, $\Omega = 0.3$ and $\delta J = 0.15$) at the lower boundary made of sites without the nearest neighbor hopping (the bottom one in Figure a). The red and blue dots mark the regions where nonlinear solutions in the form of bright and dark solitons are sought in our numerical calculations. The band structure beyond the edge of the first Brillouin zone at $\pi/2$ is shown for better display of the topological edge state dispersion.

Let $n = n_e$ is the band index corresponding to one of the TEM dispersions, see Fig. 1b. Then, solution to the full problem (2) can be sought in the form of a wavepacket centered around k_e ,

$$\boldsymbol{\psi}_m^\sigma(k_e, t) = \sum_n \int_{-\pi/L}^{\pi/L} A_n(\kappa, t) \mathbf{u}_{k_e+\kappa, n}^\sigma e^{i(k_e+\kappa)Lm} d\kappa \approx \int_{-\pi/L}^{\pi/L} A(\kappa, t) \mathbf{u}_{k_e+\kappa, n_e}^\sigma e^{i(k_e+\kappa)Lm} d\kappa \quad (4)$$

where we assumed that the single TEM with amplitude $A(\kappa, t)$ dominates other modes. For the amplitude $A(\kappa, t)$ to be uniquely defined, one needs to fix a gauge of the basis functions $\mathbf{u}_{k, n_e}^\sigma$. It is always possible to choose a gauge such that

$$\sum_\sigma \langle \mathbf{u}_{k, n_e}^\sigma, \frac{\partial}{\partial k} \mathbf{u}_{k, n_e}^\sigma \rangle = 0 \quad (5)$$

is satisfied at least within an arbitrary open interval of k smaller than the Brillouin zone. While the real part of (5) is guaranteed by the normalization, the imaginary part of (5) can be forced by the performing the $U(1)$ rotation of the eigenfunction phases. Substituting (4) to (2) and forming a scalar product with $\mathbf{u}_{k_e, n_e}^\sigma$ we get

$$\int_{-\pi/L}^{\pi/L} \sum_\sigma \left[\left(i \frac{\partial A(\kappa, t)}{\partial t} - \mu_{k_e+\kappa, n_e} A(\kappa, t) \right) \langle \mathbf{u}_{k_e, n_e}^\sigma, \mathbf{u}_{k_e+\kappa, n_e}^\sigma \rangle - A(\kappa, t) \langle \mathbf{u}_{k_e, n_e}^\sigma, \hat{N}^\sigma(\boldsymbol{\psi}_m^+, \boldsymbol{\psi}_m^-) \mathbf{u}_{k_e+\kappa, n_e}^\sigma \rangle \right] e^{i\kappa Lm} d\kappa = 0 \quad (6)$$

for all m . The condition (5) together with the completeness of the basis functions imply that the derivative $\partial \mathbf{u}_{k, n_e}^\sigma / \partial k$ comprises excitations of all other bands but n_e (in general, the bulk bands and the other TEM branches),

$$\frac{\partial}{\partial k} \mathbf{u}_{k, n_e}^\sigma = \sum_{n \neq n_e} c_n \mathbf{u}_{k, n_e}^\sigma. \quad (7)$$

Also, by differentiating (5) we get,

$$\sum_\sigma \langle \frac{\partial}{\partial k} \mathbf{u}_{k, n_e}^\sigma, \frac{\partial}{\partial k} \mathbf{u}_{k, n_e}^\sigma \rangle + \sum_\sigma \langle \mathbf{u}_{k, n_e}^\sigma, \frac{\partial^2}{\partial k^2} \mathbf{u}_{k, n_e}^\sigma \rangle = 0 \quad (8)$$

Expanding $\mathbf{u}_{k_e+\kappa, n_e}^\sigma$ into the Maclaurin series in κ , we have, from (7) and (8),

$$\sum_{\sigma} \langle \mathbf{u}_{k_e, n_e}^\sigma, \mathbf{u}_{k_e+\kappa, n_e}^\sigma \rangle \approx 1 - \frac{1}{2} \kappa^2 \sum_n |c_n|^2 \quad (9)$$

Assuming the excitation of bands $n \neq n_e$ is weak, which is guaranteed by the large energy separation of the band n_e from the rest of the bands, we can neglect the contribution of the bulk bands in (6). Decomposing $\mu_{k_e+\kappa, n_e}$ into Maclaurin series up to the 2nd order in κ and integrating, the Eq. (6) is reduced to

$$i \frac{\partial \tilde{A}}{\partial t} = \sum_{n=0}^{\infty} \frac{(-i)^n}{n!} \mu_{k_e}^{(n)} \frac{\partial^n \tilde{A}}{\partial x^n} \Big|_{x=Lm} + g |\tilde{A}|^2 \tilde{A} \quad \text{for all } x = Lm, \quad (10)$$

where

$$\tilde{A}(x, t) \equiv \int_{-\pi/L}^{\pi/L} A(\kappa, t) e^{i\kappa x} d\kappa$$

is a function of time and continuous variable x , and

$$g \equiv \sum_{\sigma} \langle \mathbf{u}_{k_e, n_e}^\sigma, \hat{N}^\sigma(\mathbf{u}_{k_e, n_e}^+, \mathbf{u}_{k_e, n_e}^-) \mathbf{u}_{k_e, n_e}^\sigma \rangle$$

is the effective nonlinearity parameter. For $\alpha \geq -1$, which is the usual case for polariton interactions³⁸, g can be proved to take non-negative values only, $g \geq 0$, irrespective of $\mathbf{u}_{k_e, n_e}^\sigma$, thus describing the defocusing nonlinearity. Finally,

$$\Psi_m^\sigma(k_e, t) \approx \tilde{A}(Lm, t) e^{ik_e Lm} \mathbf{u}_{k_e, n_e}^\sigma \quad (11)$$

Using (9), we can analyze the validity of the applied approximation. Forming the dot product of (4) with $\mathbf{u}_{k_e, n_e}^\sigma$ we obtain the constraint on the 2nd derivative of the envelope function and the level of excitation of the bulk, or other TEM, bands,

$$\left| \frac{\partial^2 \tilde{A}(x, t)}{\partial x^2} \right| \sum_n |c_n|^2 \ll |\tilde{A}(x, t)| \quad (12)$$

Note, that the obvious requirement of the independence of (11) of the choice of the kagome strip unit cell (note, that the choice of the unit cell in Fig. 1 is not unique) requires that either $\tilde{A}(x, t)$ depends weakly on x , or, there is a strong localization of the edge mode $\mathbf{u}_{k_e, n_e}^\sigma$ near the boundary within the first few rows.

Topological Edge Solitons

If the higher order terms in (10) can be neglected, the equation can be further reduced to the standard nonlinear Schrödinger (NLS) equation. Disregarding the terms $n > 2$ the solution to (10) takes the form

$$\tilde{A}(x, t) = \exp \left\{ -i\mu_{k_e} t + i \frac{(v - \mu_{k_e}')}{\mu_{k_e}''} \left[x - \frac{1}{2} (v + \mu_{k_e}') t \right] \right\} a(x - vt, t), \quad (13)$$

where v is an arbitrary real parameter, and $a(x, t)$ satisfies the NLS equation

$$i \frac{\partial a}{\partial t} + \frac{1}{2} \mu_{k_e}'' \frac{\partial^2 a}{\partial x^2} - g |a|^2 a = 0 \quad (14)$$

Note that (13) takes a form of Galilean transformation on the solution $a(x, t)$ of the NLS equation, thus introducing dynamics of the NLS solution $a(x, t)$ with velocity v . For $\mu_{k_e}'' < 0$ Eq. (14) allows solutions in the form of bright soliton (see, e.g. Ref. 39),

$$a_{\text{bright}}(x, t) = \frac{\eta e^{-i\frac{1}{2}\eta^2 g t}}{\cosh \left(\eta \sqrt{\frac{g}{|\mu_{k_e}''|}} x \right)} \quad (15)$$

where η is an arbitrary real parameter. For $\mu_{k_e}'' > 0$, there arise dark,

$$a_{\text{dark}}(x, t) = \eta e^{-i\eta^2 g t} \tanh \left[\eta \sqrt{\frac{g}{\mu_{k_e}''}} x \right] \quad (16)$$

or, more general, grey solitons

$$a_{\text{grey}}(x, t) = \eta e^{-i\eta^2 g t} \left\{ \cos \theta + i \sin \theta \tanh \left[\left(\sqrt{\frac{g}{\mu''_{k_e}}} x + \eta \cos \theta g t \right) \eta \sin \theta \right] \right\} \quad (17)$$

where η and θ are real parameters³⁹. Note, that the grey soliton envelope (17) introduces a phase shift $2|\theta|\text{sgn}(\eta)$ between the limiting points $x \rightarrow \pm\infty$. As seen from (13), the parameter v plays role of the soliton velocity for the bright and dark solitons of the Eq. (10), while the velocity of grey soliton, upon the transformation (13) is

$$v_{\text{grey}} = v - \eta \sqrt{g \mu''_{k_e}} \cos \theta. \quad (18)$$

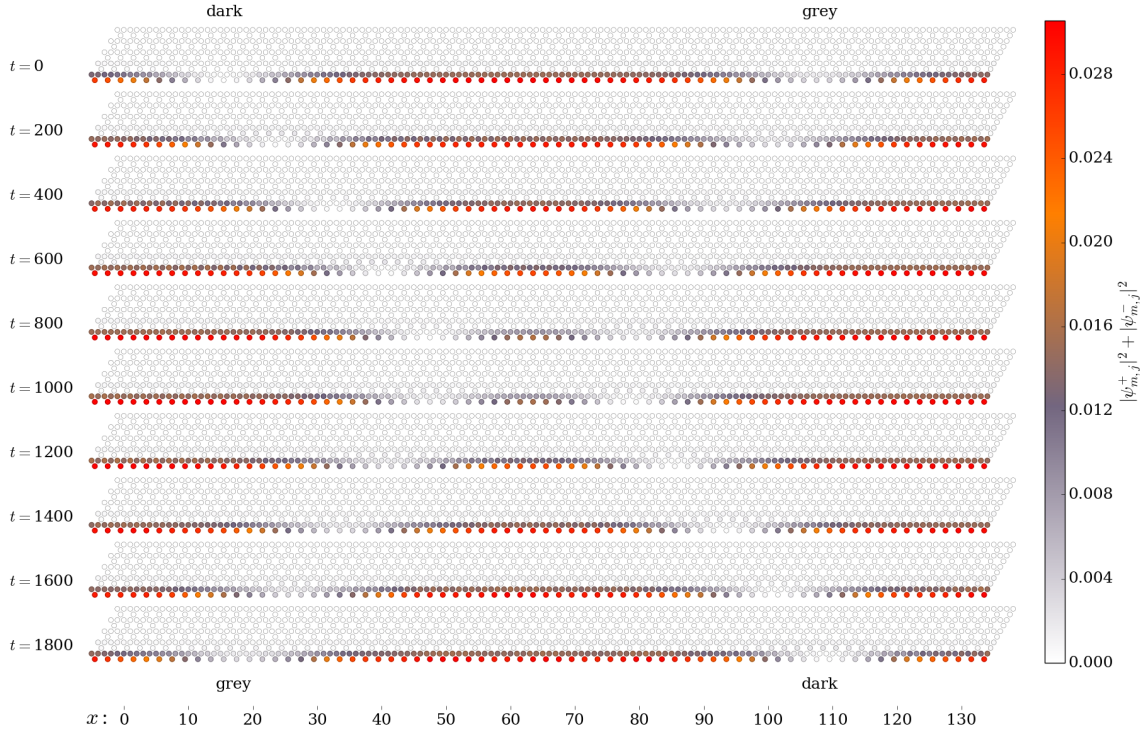


Figure 2. (Color online) Simulation of collision of dark and grey solitons excited on the TEM propagating along the lower boundary of the kagome lattice strip in Fig. 1a. The TEM is excited at quasimomentum $k_e \approx 1.59$, $E(k_e) \approx -1.09$ at $\delta J = 0.15$, $\Omega = 0.3$, in the vicinity of the blue spot on Fig. 1b. At $t = 0$ initial conditions in the form of dark (16) (on the left) and grey (17) soliton (on the right) with $\eta = 0.25$ have been taken upon applying the transformation (13) with $v \approx 0.042$. The grey soliton parameter θ was taken to be 0.4π . At $t > 0$ the dark and grey move with constant velocities until the scattering act occurs at $t \sim 1000$, following which the dark and grey solitons exchange sides.

Numerical results

We have performed simulations of the dynamics of topological edge solitons by solving the mean field model (2) numerically. Our numerical calculations confirm the appearance of a bright soliton of the type (15) whose velocity depends on the choice of the soliton momentum k_e with respect to the peak of the TEM dispersion on Fig. 1b. However, due to the strong third derivative μ'''_{k_e, n_e} of the dispersion near the maximum, the NLS (14) and the formula (15) is not applied, thus forcing one to resort to the full theory (6) and (10), unless a very extended soliton profile $\tilde{A}(x, t)$ is chosen. On the other hand, a nearly perfect parabolic dependence occurs near the edge of the first Brillouin zone at $k_e \approx \pi/2$, near the minimum of the TEM dispersion on Fig. 1b. Due to the positive second derivative $\mu''_{k_e, n_e} > 0$, and a negligible third derivative μ'''_{k_e, n_e} , it is the region where dark and grey solitons in the form (16) and (17) can be observed.

In our numerical simulations of the dark and grey solitons on Fig. 2, the TEM is excited at $k_e \approx 1.59$, $E(k_e) \approx -1.09$, $\delta J = 0.15$, $\Omega = 0.3$, in the vicinity of the blue spot on Fig. 1b. The TEM dispersion μ_{k, n_e} and the eigenstate $\mathbf{u}_{k_e, n_e}^\sigma$ were found

by solving numerically the linear problem. At the chosen value of k_e , the second derivative of the dispersion is $\mu''_{k_n, n_e} \approx 3.06$ and the nonlinearity parameter $g \approx 0.33$ where we assumed $\alpha = -0.05$ which is a typical case for the polariton-polariton interactions. At the initial time $t = 0$, the TEM is tempered by the dark and grey soliton envelopes according to the (11), (13) with soliton profiles given by (16) and (17) with parameter $\eta = 0.25$, and excited at a distance from each other. The Galilean transformation (13) has been applied with the velocity parameter $v \approx 0.042$, forcing the dark soliton to move to the right with velocity $v_{dark} = v$ according to (13). The parameter θ for the grey soliton was taken to be 0.4π which results in a grey soliton moving to the left with velocity $v_{grey} \approx -0.036$ upon transformation (13), according to (18). As seen from our numerical calculations on Fig. 2, at $t > 0$ the dark and grey solitons move with constant velocities as set by (13), (16) and (17) while keeping their shapes during propagation. Upon reaching $t \sim 1000$, scattering act occurs upon which dark and grey solitons change sides, see Fig. 2. It is interesting to note, that no actual passing of solitons *through* each other occurs. Instead, the interacting solitons stop at a distance from each other while exchanging their phase shifts. Upon the interaction has happened, the emerged dark soliton propagates to the right, while the new grey soliton keeps propagating to the left.

Discussion

Because the studied nonlinear topological edge excitations are formed from the TEM with energies inside the bulk gap, the arising solitons are robust against interaction with the bulk modes. Note, that bright topological edge solitons arising here should be distinguished from the gap solitons. Being formed from topological edge modes, bright topological edge solitons can only propagate along the boundaries of the lattice, in contrast to gap solitons, which propagate inside the bulk.

We predict that in the setting presented here it will be easier to detect experimentally dark and grey solitons rather than the bright ones. Indeed, as seen from Fig. 1b, at a fixed k_e the separation from the bulk modes is much larger for the minimum of the TEM dispersion (at $k_e \approx \pi/2$) as opposed to the maximum of the TEM dispersion (at $k_e \approx 1.3$). Therefore, the criterion (12) is much more likely to be satisfied for the dark/grey soliton regime. As an example, at $k \approx \pi/2$ and the typical coupling strength $J = 1$ meV, the separation between the $n_e - 1$ and $n_e + 1$ bands amounts 1.2 meV in physical units. Moreover, these estimates show that, as soon as scattering to other k -modes at a given energy can be neglected, it is not necessary to open a large gap in the dispersion relation for the topological edge dark and grey solitons to be detected experimentally.

References

1. Georgescu, I., Ashhab, S. & Nori, F. Quantum simulation. *Reviews of Modern Physics* **86**, 153 (2014).
2. Kane, C. L. & Mele, E. J. Quantum spin hall effect in graphene. *Phys. Rev. Lett.* **95**, 226801 (2005).
3. Bernevig, B. A., Hughes, T. L. & Zhang, S. C. Quantum spin hall effect and topological phase transition in hgte quantum wells. *Science* **314**, 1757 (2006).
4. König, M. *et al.* Quantum spin hall insulator state in hgte quantum wells. *Science* **318**, 766 (2007).
5. Raghu, S. & Haldane, F. D. M. Analogs of quantum-hall-effect edge states in photonic crystals. *Phys. Rev. A* **78**, 033834 (2008).
6. Haldane, F. & Raghu, S. Possible realization of directional optical waveguides in photonic crystals with broken time-reversal symmetry. *Phys. Rev. Lett.* **100**, 013904 (2008).
7. Wang, Z., Chong, Y., Joannopoulos, J. D. & Soljačić, M. Reflection-free one-way edge modes in a gyromagnetic photonic crystal. *Phys. Rev. Lett.* **100**, 013905 (2008).
8. Wang, Z., Chong, Y., Joannopoulos, F. D. & Soljačić, M. Observation of unidirectional backscattering-immune topological electromagnetic states. *Nature* **461**, 772–775 (2009).
9. Hafezi, M., Demler, E. A., Lukin, M. D. & Taylor, J. M. Robust optical delay lines with topological protection. *Nature Physics* **7**, 907–912 (2011).
10. Fang, K., Yu, Z. & Fan, S. Realizing effective magnetic field for photons by controlling the phase of dynamic modulation. *Nature Photonics* **6**, 782 (2012).
11. Rechtsman, M. C. *et al.* Photonic floquet topological insulators. *Nature* **496**, 196 (2013).
12. Khanikaev, A. B. *et al.* Photonic topological insulators. *Nature Materials* **12**, 233–239 (2013).
13. Lu, L., Joannopoulos, J. D. & Soljačić, M. Topological photonics. *Nature Photonics* **8**, 821 (2014).
14. Carusotto, I. & Ciuti, C. Quantum fluids of light. *Reviews of Modern Physics* **85**, 299 (2013).
15. Cerda-Méndez, E. A. *et al.* Polariton condensation in dynamic acoustic lattices. *Phys. Rev. Lett.* **105**, 116402 (2010).

16. Kim, N. Y. *et al.* Exciton–polariton condensates near the dirac point in a triangular lattice. *New Journal of Physics* **15**, 035032.
17. Jacqumin, T. *et al.* Direct observation of dirac cones and a flatband in a honeycomb lattice for polaritons. *Phys. Rev. Lett.* **112**, 116402 (2014).
18. Baboux, F. *et al.* Bosonic condensation and disorder-induced localization in a flat band. *Phys. Rev. Lett.* **116**, 066402 (2016).
19. Liew, T., Shelykh, I. & Malpuech, G. Polaritonic devices. *Physica E*.
20. D. Sanvitto, D. & Kéna-Cohen, S. The road towards polaritonic devices. *Nature Materials* **15**.
21. Karzig, T., Bardyn, C.-E., Lindner, N. H. & Refael, G. Topological polaritons. *Phys. Rev. X* **5**, 031001 (2015).
22. Bardyn, C.-E., Karzig, T., Refael, G. & Liew, T. C. H. Topological polaritons and excitons in garden-variety systems. *Phys. Rev. B* **91**, 161413 (2015).
23. Nalitov, A. V., Solnyshkov, D. D. & Malpuech, G. Polariton \mathbb{Z} topological insulator. *Phys. Rev. Lett.* **114**, 116401 (2015).
24. Yi, K. & Karzig, T. Topological polaritons from photonic dirac cones coupled to excitons in a magnetic field. *Phys. Rev. B* **93**, 104303 (2016).
25. Bardyn, C.-E., Karzig, T., Refael, G. & Liew, T. C. H. Chiral bogoliubov excitations in nonlinear bosonic systems. *Phys. Rev. B* **93**, 020502 (2016).
26. Janot, A., Rosenow, B. & Refael, G. Topological polaritons in a quantum spin hall cavity. *Phys. Rev. B* **93**, 161111 (2016).
27. Gulevich, D. R., Yudin, D., Iorsh, I. V. & Shelykh, I. A. Kagome lattice from an exciton-polariton perspective. *Phys. Rev. B* **94**, 115437 (2016).
28. Lumer, Y., Plotnik, Y., Rechtsman, M. C. & Segev, M. Self-localized states in photonic topological insulators. *Phys. Rev. Lett.* **111**, 243905 (2013).
29. Ostrovskaya, E. A., Abdullaev, J., Fraser, M. D., Desyatnikov, A. S. & Kivshar, Y. S. Self-localization of polariton condensates in periodic potentials. *Phys. Rev. Lett.* **110**, 170407 (2013).
30. Hadad, Y., Khanikaev, A. B. & Alù, A. Self-induced topological transitions and edge states supported by nonlinear staggered potentials. *Phys. Rev. B* **93**, 155112 (2016).
31. Kartashov, Y. V. & Skryabin, D. V. Two-dimensional lattice solitons in polariton condensates with spin-orbit coupling. *Opt. Lett.* **41**, 5043–5046 (2016).
32. Gulevich, D. R., Skryabin, D. V., Alodjants, A. P. & Shelykh, I. A. Topological spin meissner effect in spinor exciton-polariton condensate: Constant amplitude solutions, half-vortices, and symmetry breaking. *Phys. Rev. B* **94**, 115407 (2016).
33. Ablowitz, M. J., Curtis, C. W. & Ma, Y.-P. Linear and nonlinear traveling edge waves in optical honeycomb lattices. *Phys. Rev. A* **90**, 023813 (2014).
34. Leykam, D. & Chong, Y. D. Edge solitons in nonlinear-photonic topological insulators. *Phys. Rev. Lett.* **117**, 143901 (2016).
35. Kartashov, Y. V. & Skryabin, D. V. Modulational instability and solitary waves in polariton topological insulators. *Optica* **3** 1228 (2016).
36. Cerda-Méndez, E. A. *et al.* Exciton-polariton gap solitons in two-dimensional lattices. *Phys. Rev. Lett.* **111**, 146401 (2013).
37. Rajaraman, R. *Solitons and Instantons: An Introduction to Solitons and Instantons in Quantum Field Theory* (Elsevier Science, 1987).
38. Vladimirova, M. *et al.* Polarization controlled nonlinear transmission of light through semiconductor microcavities. *Phys. Rev. B* **79**, 115325 (2009).
39. Ablowitz, M. J. *Nonlinear Dispersive Waves: Asymptotic Analysis and Solitons* (Cambridge University Press, 2011).

Acknowledgements

D.Y. acknowledges support from RFBR project 16-32-60040. I.I. acknowledges support from RFBR Project 15-02-08949. I.A.S. and I.I. acknowledge support from Rannis projects 141241-051 and 163082-051. D.V.S acknowledges support from ITMO University through the grant of the Government of the Russian Federation (074-U01).